# LABEL-FREE VOLTAMMETRIC DETECTION OF PRODUCTS OF TERMINAL DEOXYNUCLEOTIDYL TRANSFERASE TAILING REACTION

Monika Hermanová[1], Pavlína Havranová-Vidláková[1], Anna Ondráčková[1], Swathi Senthil Kumar[2], Richard Bowater[2], Miroslav Fojta[1,3,*]

*[1] Institute of Biophysics, Czech Academy of Sciences, Kralovopolska 135, 612 65 Brno, Czech Republic*

*[2] School of Biological Sciences, University of East Anglia, Norwich, Norwich Research Park, NR4 7TJ, United Kingdom*

*[3] Central European Institute of Technology, Masaryk University, Kamenice 753/5, CZ-625 00 Brno, Czech Republic*

**\***Corresponding author: fojta@ibp.cz

**Abstract**

A label-free approach that takes advantage of intrinsic electrochemical activity of nucleobases has been applied to study the products of terminal deoxynucleotidyl transferase (TdT) tailing reaction. DNA homooligonucleotides $A_{30}$, $C_{30}$ and $T_{30}$ were used as primers for the tailing reaction to which a dNTP - or a mixture of dNTPs - and TdT were added to form the tails. Electrochemical detection enabled study of the tailing reaction products created by various combinations of primers and dNTPs, with pyrolytic graphite electrode (PGE) being suitable for remarkably precise analysis of the length of tailing reaction products. Furthermore, the hanging mercury drop electrode (HMDE) was able to reveal formation of various DNA structures, such as DNA hairpins and G-quadruplexes, which influence the behavior of DNA molecules at the negatively charged surface of HMDE. Thus, the described approach proves to be an excellent tool for studying the TdT tailing reactions and for exploring how various DNA structures affect both the tailing reactions and electrochemical behavior of DNA oligonucleotides at electrode surfaces.

## 1. Introduction

Terminal Deoxynucleotidyl Transferase (TdT) is a unique DNA polymerase as it catalyzes random polymerization of deoxynucleotides at the 3'-OH ends of DNA in a template independent manner [1,2]. The physiological role of TdT lies in random addition of nucleotides to single-stranded DNA during V(D)J recombination. The ability of TdT to randomly incorporate nucleotides increases antigen receptor diversity and, thus, TdT plays a crucial role in the evolution and adaptation of the vertebrate immune system [3]. For its catalytic activity, the enzyme requires a free 3'-OH group and a minimum of three nucleotide residues to constitute the primer [4]. *In vitro*, TdT can incorporate all four natural deoxyribonucleotides into single-stranded DNA. However, *in vivo*, a bias was observed towards the incorporation of pyrimidine versus purine nucleotides [2], with the incorporation efficiency of G being more than 4-fold higher than that of A [5,6]. TdT, like all DNA polymerases, requires divalent metal ions for the catalysis. However, TdT is unique in its ability to use a variety of divalent cations, such as $Co^{2+}$, $Mn^{2+}$, $Zn^{2+}$ and $Mg^{2+}$ [7]. Each metal ion has different effects on the kinetics and mechanism of dNTP (deoxynucleoside triphosphates; N stands for A, adenine, C, cytosine, G, guanine or T, thymine) utilization. For example, $Mg^{2+}$ facilitates the preferential utilization of dGTP and dATP whereas $Co^{2+}$ increases the catalytic polymerization efficiency of the pyrimidines, dCTP and dTTP [8].

Nucleic acids are electrochemically active, which was first shown in the second half of the 1950s [9], and yield analytically useful signals at various electrodes [10,11]. Mercury-based electrodes (such as hanging mercury drop electrode, HMDE) are traditionally used to measure DNA signals related to reduction of its natural components (although it should be noted that reduction of nucleobases at a graphite electrode has recently been reported on [12]). Here, we use the HMDE as a well-established tool for DNA structure-sensitive measurements. In mixed nucleotide sequences, adenine (A) and cytosine (C) yield the common cathodic CA peak resulting from their reduction; guanine (G) gives the anodic $G^{HMDE}$ peak, which results from re-oxidation of a reduction product of guanine, 7,8-dihydroguanine, which is formed at very negative potentials and, therefore, cannot be observed under usually applied conditions due to an overlap of its signal with the cathodic background discharge at the mercury electrode [13,14]. At carbon electrodes, A and G can be oxidized at positive potentials, giving rise to $A^{OX}$ and $G^{OX}$ peaks, respectively. Analogues of natural purines, 7-deazaadenine (A*) and 7-deazaguanine (G*), can also be studied using carbon electrodes as they produce oxidation signals at positive potentials [15]. Moreover, adsorption/desorption processes or reorientation of parts of the DNA chains occur at the negatively charged surface of mercury electrodes, which can be observed as tensammetric (capacitive) signals [10]. Generally, signals gained at mercury-containing electrodes are remarkably sensitive to changes in DNA structure, which enables detection of different types of changes, such as formation of strand breaks [16], DNA superhelicity-induced structural transitions [17], binding of DNA intercalators [18] or formation of non-canonical DNA structures such as triplexes [19] and quadruplexes [20,21].

Methods for studying the TdT tailing reaction have been based on polyacrylamide gel electrophoresis (PAGE), usually along with radioactive labeling of DNA [22–27]. Here, for the first time we apply an electrochemistry-based approach to study the TdT tailing reactions,

taking advantage of the intrinsic electroactivity of nucleobases. A set of DNA homooligonucleotides were used as primers for the tailing reactions, to which a dNTP (or a mixture of dNTPs) and TdT were added to form the tails. Taking account of the primer and dNTP used in the particular reaction, an appropriate electrode was chosen for the tailing reaction products analysis - HMDE or pyrolytic graphite electrode (PGE). We show that electrochemical analysis enables a very precise study of the TdT tailing reaction products and, furthermore, it can detect formation of DNA structures occurring in the TdT products.

## 2. Experimental section

### 2.1 Terminal Deoxynucleotidyl Transferase (TdT) reaction

As primers for the TdT reaction, single stranded oligonucleotides composed of one nucleotide type, $A_{30}$, $C_{30}$ and $T_{30}$ (Generi Biotech, Czech Rep.) were used. The reaction mixture contained 5 µM DNA primer ($A_{30}$, $C_{30}$ or $T_{30}$), 5 µM, 25 µM, 50 µM, 100 µM or 250 µM dNTP (dGTP, dG*TP, dATP, dA*TP, dCTP or dTTP, Sigma-Aldrich, USA), 10 U Terminal Deoxynucleotidyl Transferase (calf thymus, recombinant expressed in *E. coli*; New England Biolabs, USA) and 250 µM $CoCl_2$ in a total volume of 20 µl. Reaction mixtures were incubated at 37 °C for 60 min. Products of the TdT reaction were purified using the Nucleotide Removal Kit (Qiagen, the Netherlands) and dissolved in 30 µl deionized water.

### 2.2 Denaturing PAGE

TdT reaction products were labeled by ^{32}P, dried out and dissolved in 5 µl loading buffer (80% formamide, 10 mM EDTA, 1 mg.ml^{-1} xylene cyanol FF, 1 mg.ml^{-1} bromphenol blue). Aliquots (2.5 µl) of the reaction mixtures were loaded into a 15% denaturing polyacrylamide gel containing 1x TBE pH 8 and 7 M urea, which had been preheated at 25 W for 30 min, and then electrophoresis continued at 25 W for 90 min. After drying, the gel was autoradiographed and visualized using a Typhoon FLA 9000.

### 2.3 Electrochemical analysis

All electrochemical measurements were performed at room temperature in a three-electrode setup (with the hanging mercury drop electrode, HMDE, or basal-plane pyrolytic graphite electrode, PGE, as the working electrode, Ag/AgCl/3 M KCl as the reference electrode and platinum wire as the auxiliary electrode) using an Autolab analyzer (Ecochemie, the Netherlands) in connection with VA-Stand 663 (Metrohm, Switzerland). The measurements were done in an adsorptive transfer stripping (AdTS) mode. DNA (10 µg.ml^{-1}) was accumulated at the electrode surface from 4 µl aliquots (containing 0.2 M NaCl) for 60 s, then the electrode was rinsed by deionized water and placed into the electrochemical cell containing blank electrolyte. Cyclic voltammetry (CV) measurements at HMDE were performed in 0.3 M ammonium formate with 0.05 M sodium phosphate, pH 6.9 as electrolyte; CV settings were: initial potential 0.0 V, switching potential -1.85 V, final potential 0.0 V, scan rate 1 V.s^{-1}, step potential 5 mV. Before each CV measurement the solution of the background electrolyte was purged with argon. Square wave voltammetry (SWV) measurements at PGE were performed in 0.2 M acetate buffer, pH 5.0; SWV settings were:

initial potential -1 V, final potential 1.6 V, frequency 200 Hz, amplitude 50 mV, scan rate 1 $V.s^{-1}$. Before each SWV measurement the PGE was pretreated by applying a potential of 1.8 V for 30 s in the background electrolyte, and its surface was renewed by peeling off the graphite top layer using sticky tape.

## 3. Results and discussion

For the tailing reaction, three types of homooligonucleotides – $A_{30}$, $C_{30}$ and $T_{30}$ – were used as primers to which various dNTPs (dATP, dCTP, dGTP, dTTP, 7-deazaadenine - dA*TP and 7-deazaguanine - dG*TP or their combinations) were added to form the tail. $G_{30}$ was not used as a primer since DNA oligonucleotides containing longer stretches of guanines tend to form G-quadruplexes (G4) [21,28] and such structure would not be a suitable substrate for TdT because of its inability to access the 3'-OH end folded within the G4 structure. Figure 1 shows cyclic voltammograms at HMDE and square wave voltammograms at PGE gained for the $A_{30}$, $C_{30}$ and $T_{30}$ primers compared to blank electrolyte. For the $A_{30}$ primer, the A reduction peak at HMDE ($A^{HMDE}$) and A oxidation peak at PGE ($A^{OX}$) can be observed. $C_{30}$ yields only a reduction peak at HMDE. No faradaic signals can be observed for $T_{30}$ at HMDE or PGE under these conditions. However, with HMDE, a tensammetric peak ($T^{TENS}$) resulting from the desorption and reorientation processes of $T_{30}$ and taking place at negative potentials (around -1.5 V) at mercury electrode surface is evident. This behavior of oligo(dT) has been described previously [29]. Both cyclic and square wave voltammograms of the individual primers show that when measuring the particular homooligonucleotide primer, signals of no other bases are visible, which means that after choosing an appropriate combination of primer and dNTP, the primers can be used for monitoring the TdT tailing reaction. The TdT tailing reaction was performed in five different dNTP:primer molar ratios: 1:1, 5:1, 10:1, 20:1 and 50:1; a "no enzyme" control was performed in order to compare signals gained for the tailing reaction products to those of the sole primer and to exclude interference of dNTP residues possibly present in the tailing product solutions.
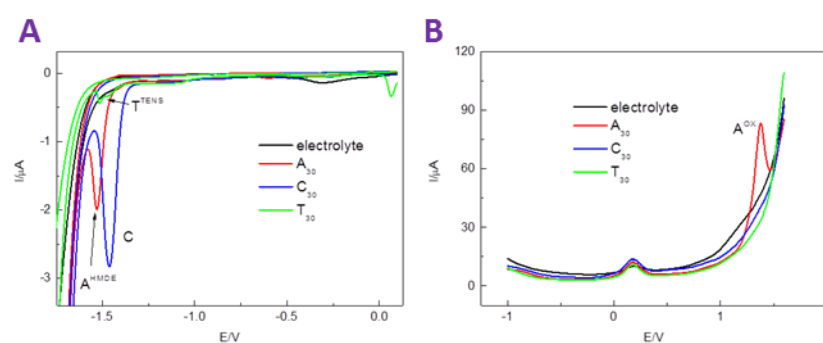


Figure 1. Cyclic voltammograms at HMDE (A) and square wave voltammograms at PGE (B) of the $A_{30}$, $C_{30}$ and $T_{30}$ primers. Signals yielded by individual primers are labelled.
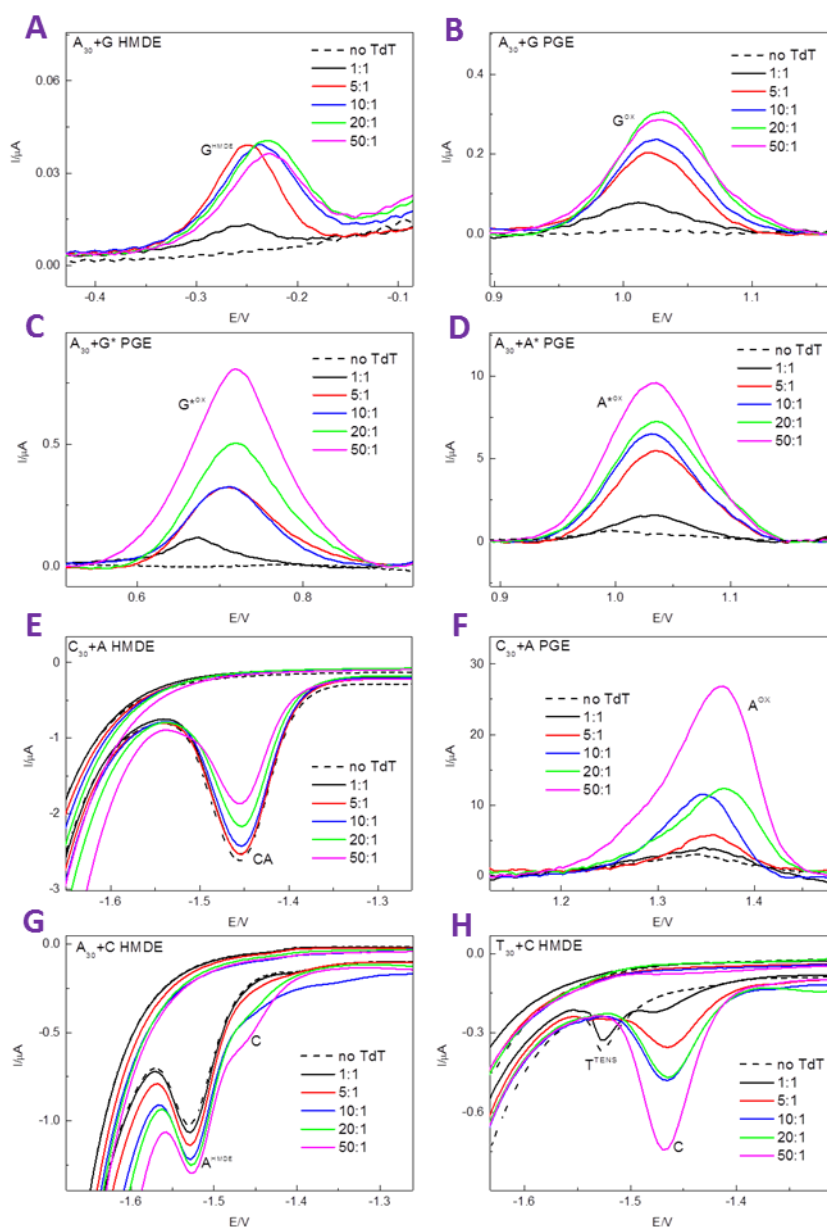
Figure 2. Examples of sections of cyclic (obtained at HMDE) and square wave (obtained at PGE) voltammograms gained for various combinations of primers and dNTPs: (A) $A_{30}$+G HMDE; (B) $A_{30}$+G PGE; (C) $A_{30}$+G* PGE; (D) $A_{30}$+A* PGE; (E) $C_{30}$+A HMDE; (F) $C_{30}$+A PGE; (G) $A_{30}$+C HMDE; (H) $T_{30}$+C HMDE. Reaction conditions and significant conclusions are discussed in the text.

Guanine (G) and 7-deazaguanine (G*) were used for the tailing reaction with all three primers - $A_{30}$, $C_{30}$ and $T_{30}$ (Figure 2). Regardless of which primer was used, the signals observed corresponded with composition of the reaction mixture i.e., for dGTP peak $G^{HMDE}$ and peak $G^{OX}$ were observed, whereas for dG*TP peak $G^{*OX}$ appeared. The $A_{30}$+G combination revealed a significant difference between the results gained at HMDE and PGE for the same reaction products (Figures 2A, B and 3A). With PGE the height of the $G^{OX}$ peak continuously increased with the increasing dNTP:primer ratio. In contrast, peak $G^{HMDE}$ showed a decreasing tendency from a 5:1 to 50:1 ratio after the initial growth between 1:1 and 5:1 ratio.

This behavior at HMDE is in contrast to what was observed at PGE. An analogous effect, decrease of peak $G^{HMDE}$ with increasing length of $G_n$ stretches, has been previously observed and ascribed to the formation of intermolecular parallel G-quadruplexes (G4) [21]. Since the G-rich sequences are generally known to adopt the structure of G4 and this ability is more pronounced in longer $G_n$ stretches, it can be assumed that the G-tails formed G4 at dNTP:primer molar ratios of 5:1 and higher. This assumption is further supported by the fact that $K^+$ ions, which stabilize formation of G4, are present in the TdT reaction buffer, in which the tailing reaction takes place.

The denaturing PAGE autoradiogram showed that the length of the tailing reaction products did not grow significantly at dGTP:primer ratios higher than 5:1. Moreover, for the ratios 5:1 and higher, heavier species were formed (detected at starts of the gel, see Figure 3A), whose mass was too big to enter the gel; these species can be expected to be formed by the intermolecular G4. This suggested that DNA obtained from the G-tailing reactions occurred in two states: G4, which were resistant to the denaturing conditions during the PAGE, and unstructured oligonucleotides that create a ladder typical for TdT tailing reaction products. In principle, formation of G4 structures influences the intensity of the measured peak $G^{HMDE}$ in two ways. Firstly, when the dNTP:primer ratio is sufficient to produce G-tails that are capable of stable G4 formation, the tailing reaction is stopped when the G4 is formed because of the inaccessibility of the 3'-OH end to TdT. Secondly, the G4 formation changes behavior of the oligonucleotides at the mercury electrode surface, which is related to the fact that DNA structures existing in solution can be preserved after adsorption at the electrode surface in adsorptive transfer techniques [10]. Moreover, mercury-containing electrodes are sensitive to changes in DNA structure. It has been well established that the accessibility of nucleobase residues for electrode reactions is strongly dependent on the DNA structure, particularly at mercury electrodes. It can be assumed that this feature is responsible for the decrease of the signals at the HMDE, together with the fact that electrostatic repulsion of the rigid quadruplex structures from the negatively charged surface of the HMDE may hinder reduction of guanine residues involved [21]. On the other hand, the oxidation of guanine at the PGE takes place at the positively charged surface of the electrode to which the oligonucleotide molecules are attracted. This facilitates the oxidation process even in the quadruplex structure. Along with bigger accessibility of the primary oxidation site of guanine to the electrode surface, the signals gained for oxidation of guanine at the PGE depend merely on the length of the oligonucleotide molecules and do not reflect any structural changes occurring in the molecules. When comparing the PAGE autoradiogram and the $G^{OX}$ peak heights at the PGE, very similar trends were observed, with a steep increase between the 1:1 and 5:1 ratio followed by a slower increase from 5:1 to 50:1 ratio. PAGE and electrochemical analysis with the PGE thus provided comparable results as to the length of the tailing reaction products, thus making the latter a suitable alternative method for studying the process of the TdT tailing reactions. On the other hand, electrochemical measurements in the negative potential region with the HMDE provide extra information about DNA structural transitions.
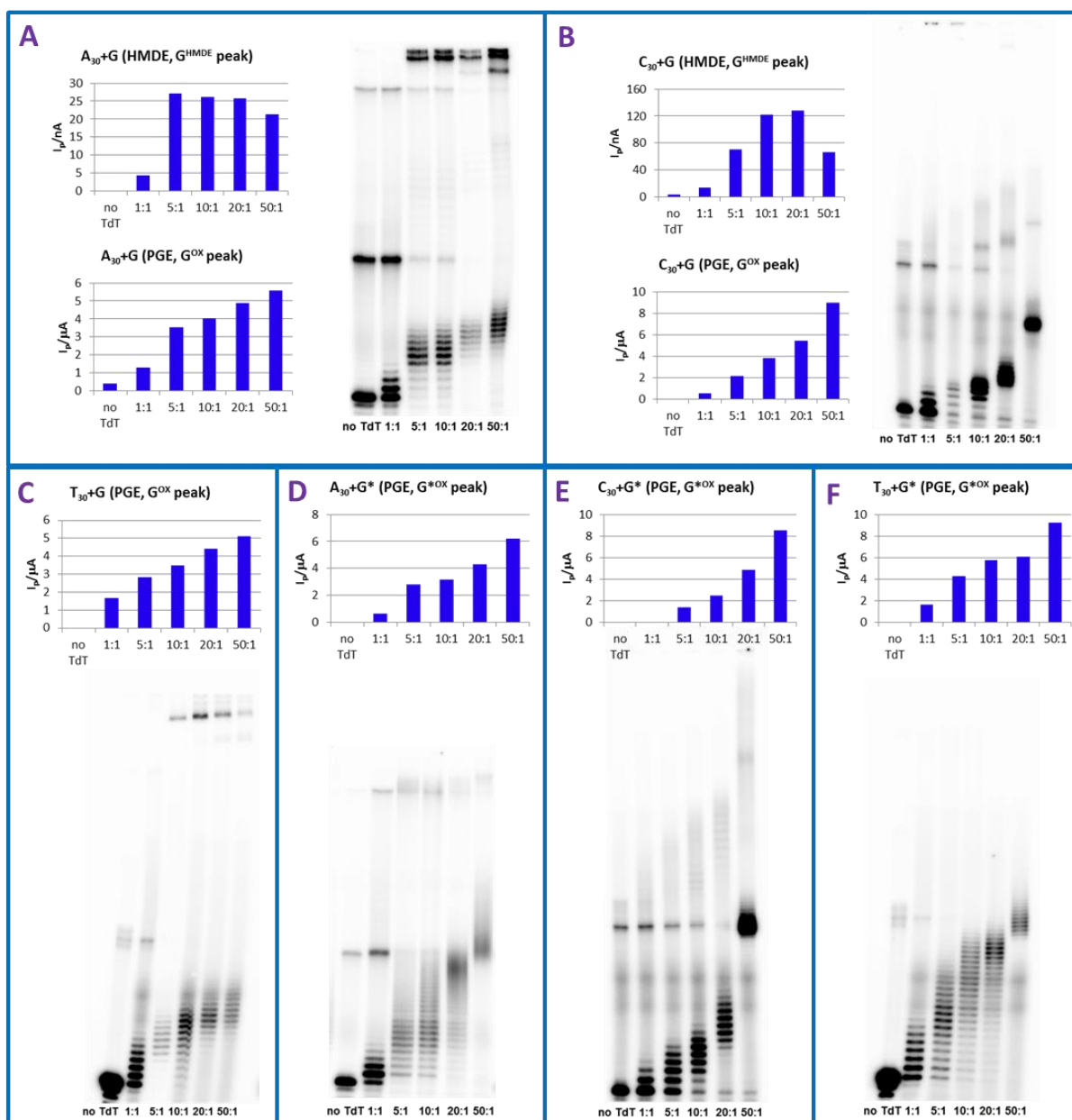
Figure 3. Heights of the respective peaks gained at HMDE or PGE and denaturing PAGE autoradiograms obtained for combinations of G and G* with all three primers: (A) $A_{30}+G$; (B) $A_{30}+C$; (C) $T_{30}+G$; (D) $A_{30}+G^*$; (E) $C_{30}+G^*$; (F) $T_{30}+G^*$. Reaction conditions and significant conclusions are discussed in the text.

In the case of $T_{30}+G$ (Figure 3C), the denaturing PAGE revealed the same pattern of the length of the tailing reaction products as $A_{30}+G$, indicating formation of G4 at ratios higher than 5:1, and a very similar trend as for $A_{30}+G$ was also observed using voltammetric analysis at PGE. Nevertheless, voltammetric responses of the $T_{30}+G$ tailing products at HMDE could not be compared to those of $A_{30}+G$ because behavior of the former at HMDE is predominantly affected by the $T_{30}$ oligonucleotide due to strong interactions of homopyrimidine stretches with the negatively charged HMDE surface [29], which can further

affect adsorption and redox processes of the G-tails, especially if G4 are formed. These phenomena, whose detailed description is out of scope of this report, are intensively studied in our laboratory (S. Hasoň, H. Pivoňková et al., manuscripts in preparation).

Unlike $A_{30}$+G and $T_{30}$+G, the $C_{30}$+G tailing reaction products (Figure 3B) did not form G4, which is evident from the PAGE autoradiogram showing that the tail length does not stop growing after a particular ratio and the longest products are obtained for the highest ratio (50:1). Voltammetric analysis at PGE again reveals a good correlation with the PAGE analysis. However, at HMDE, the signal grows only until the 20:1 ratio, then for the 50:1 ratio the signal drops significantly. This can be explained by formation of another DNA structure, such as a DNA hairpin (or, alternatively, duplex dimer of self-complementary $G_nC_m$ oligonucleotides). Bases C and G are complementary and tend to form duplex DNA when possible, therefore when the G-tail reaches sufficient length for the hairpin formation (in this case around 30 added nucleotides) it can bend over and form a hairpin with the complementary C30 primer. The formation of such alternative structures can make signals at HMDE decrease. It can also explain why only one band corresponding to two or three lengths of the tailing products occurs in the PAGE autoradiogram, suggesting that the tailing reaction stops when the DNA hairpin is formed.

For comparison with the behavior of the natural guanine, 7-deazaguanine (G*) was used, which is an analogue of natural guanine in which the N7 atom is replaced by CH group. This feature implicates that while the Watson-Crick base pairing (with C) of the 7-deazaguanine remains unaffected, the Hoogsteen base pairs cannot be formed due to the involvement of the N7 atom in the formation of this type of base pair. Thus, DNA molecules containing G* are incapable of forming multi-stranded DNA structures, such as triplexes or quadruplexes. This fact is utilized, for example, in PCR amplification of G-rich sequences where the quadruplex formation could affect the amplification process. For analysis of the $A_{30}$+G* tailing reaction products (Figure 2C and 3D), only oxidation at PGE was used since, with HMDE, G* does not yield any peak analogous to the $G^{HMDE}$ peak, in agreement with absence of the corresponding redox site in G* [30]. Both voltammetric and PAGE analysis showed that, unlike in the case of $A_{30}$+G tailing products, the length of the tailing products grew gradually with the rising dG*TP:primer ratio, with the average tail length much higher than in the case of dGTP, especially for the 20:1 and 50:1 ratios and the $G^{*OX}$ signal for the 50:1 ratio being ~10-fold higher than that for the 1:1 ratio. This was in agreement with the fact that, unlike natural guanine, G* is not capable of forming G4 and, therefore, the TdT tailing reaction was not inhibited in contrast to what was observed in experiments with G (see above). G* is thus suitable for studying how TdT incorporates an analogue of G into DNA as it does not exhibit limitations related to formation of G4 structures described above for G.

Practically the same results as for the $A_{30}$+G* were obtained for the $T_{30}$+G* tailing products (Figure 3F) with a similar pattern of the tailing products lengths visible on the PAGE autoradiogram and intensities of the $G^{*OX}$ signal gained at PGE. On the other hand, the pattern observed for $C_{30}$+G* (Figure 3E) resembled more that of the $C_{30}$+G tailing products than those of $A_{30}$+G* and $T_{30}$+G*, which is in accordance with the fact that the ability of G*

to form Watson-Crick pairs with C is not violated, which allows hairpin formation after a certain length of the tail is reached.
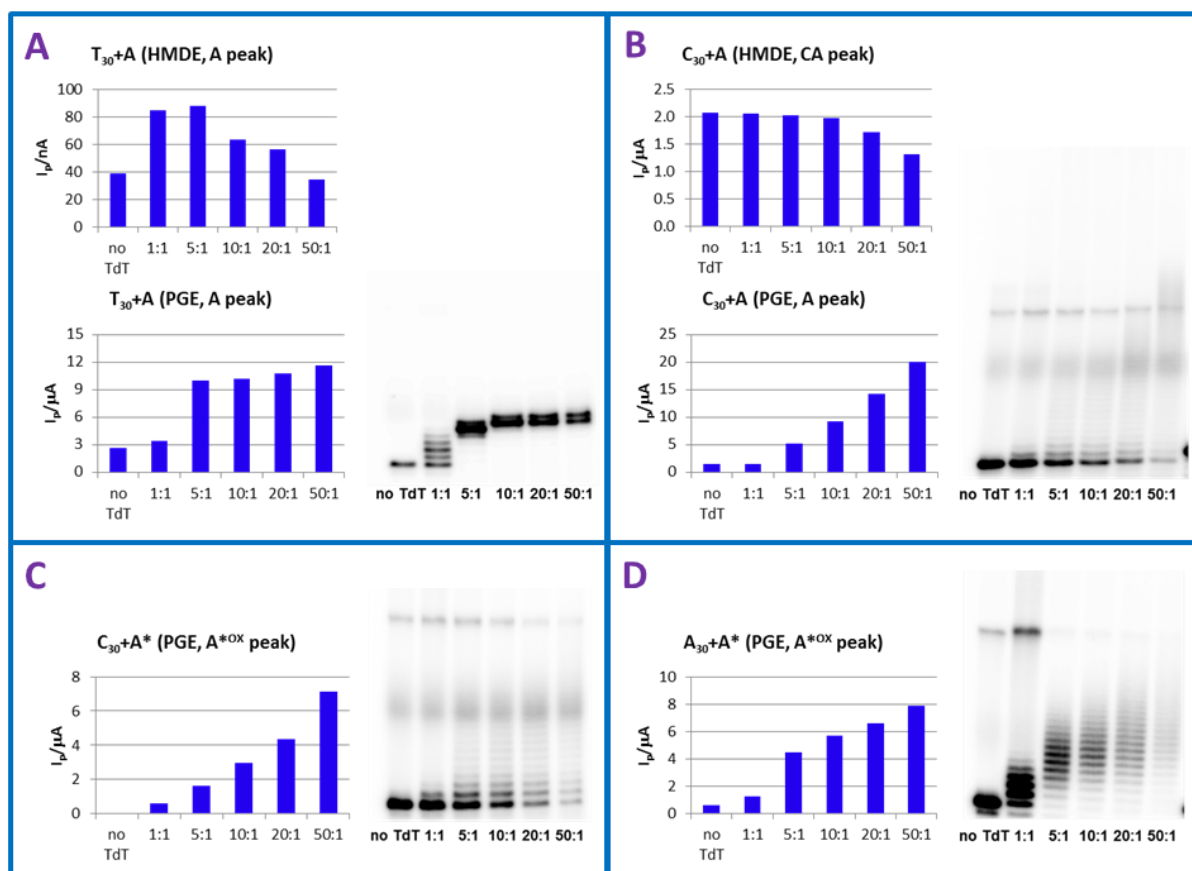


Figure 4. Heights of the respective peaks gained at HMDE or PGE and denaturing PAGE autoradiograms obtained for combinations of A and A* with all three primers: (A) $T_{30}$+A; (B) $C_{30}$+A; (C) $C_{30}$+A*; (D) $A_{30}$+A*. Reaction conditions and significant conclusions are discussed in the text.

Besides guanine and 7-deazaguanine, adenine and 7-deazaadenine (A*) were also used for the tailing reactions, together with primers $T_{30}$, $C_{30}$ and $A_{30}$ (the latter only for A*). For the $T_{30}$+A (Figure 4A), PAGE analysis revealed that for the 1:1 ratio an average of two nucleotides were added. However, starting at the 5:1 ratio, the reaction stopped after 5 or 6 added nucleotides. Therefore, all the reaction products for the ratios 5:1, 10:1, 20:1 and 50:1 had tails consisting of 5 or 6 nucleotides. This behavior might be caused by a formation of a DNA hairpin (or dimer) since A and T are complementary bases and, like C and G, they are prone to duplex creation. When the A tail reaches sufficient length for the hairpin formation, the DNA bends and a DNA hairpin with a 5' overhang is created. This means that the 3'-OH end becomes poorly accessible for the TdT and the enzyme cannot continue in the tailing reaction – at least in certain population of the tailing products. Electrochemical results obtained for the $T_{30}$+A again displayed significant difference between the data obtained at HMDE and PGE (similarly to $A_{30}$+G and $C_{30}$+G). In the cyclic voltammogram gained at HMDE, the tensammetric peak mentioned above caused by the $T_{30}$ primer can be observed. The potential of the $T^{TENS}$ peak coincides with that of $A^{HMDE}$ peak. Thus, these two peaks cannot be

distinguished and there is a non-zero value for the primer (no TdT control). Then, for the 1:1 and 5:1 ratios the height of the collective peak at -1.52 V increased in comparison to the signal gained for the sole primer, which agreed with the growing length of the A tails observed at the PAGE autoradiogram. For the higher ratios, where the DNA hairpin is expected to be formed, the signal sharply decreased, which was also observed for $C_{30}$+G and is in agreement with the fact that HMDE is sensitive to structural changes occurring in DNA. On the other hand, the signals gained at PGE generally exhibit a poor sensitivity to variations in DNA structure; therefore, the height of the $A^{OX}$ peak displays a trend very similar to that visible at the PAGE autoradiogram.

The $C_{30}$+A combination generates a specific signal for the bases forming the primer and the tail (Figure 2E,F and 4B). This occurs because in DNAs with a random distribution of bases, C and A yield a common CA peak at HMDE since their reduction potentials are in close proximity. However, in DNA composed of C and A homooligonucleotide stretches, two separated peaks can be observed under certain conditions [31–33]. In this case, it was not possible to see the separate C and $A^{HMDE}$ peaks, only a hint of the $A^{HMDE}$ peak appeared at a potential more negative than that of the C peak for the product with the longest A tail (i.e. for the 50:1 ratio). The height of the C peak decreased with the increasing dATP:primer ratio, reflecting the decreasing proportion of cytosines in the tailing products. At PGE, the intensity of the $A^{OX}$ peak increased with higher ratios of dATP:primer, but it was not possible to compare the trend of this signal to the pattern gained at PAGE since, in this case, the PAGE analysis did not show distinct bands of the tailing products. Most probably this was caused by a wider distribution of the lengths of tails, leading to smaller amounts of DNA of each specific length, meaning that the bands corresponding to such lengths could not be visualized. Nevertheless, the intensity of the band of the unextended $C_{30}$ primer decreased with the higher ratios of dATP:primer, which indicates that the primer has been consumed for the tailing reaction. The same effect can be observed at the PAGE autoradiogram of the $C_{30}$+A* tailing products (Figure 4C), again making the electrochemical analysis at PGE more accurate than the PAGE analysis. In both cases, the general trends of these signals are practically the same (unlike in the case of $A_{30}$+G), indicating that no unusual structure is formed in the A tail. Thus, we can see that in some instances electrochemical analysis at PGE responds to the increase of mean length of the tailing products more clearly than the PAGE analysis.

Results gained for the $A_{30}$+A* tailing products (Figure 2D and 4D) show that the trend of the growing tail length visible at both PAGE autoradiogram and electrochemical analysis at PGE is different from that of $C_{30}$+A* tailing products, which probably reflects different preferences of the TdT for different primers and dNTP substrates. However, again there is a striking agreement between the results of PAGE and electrochemistry with PGE for the given primer-dNTP pair.
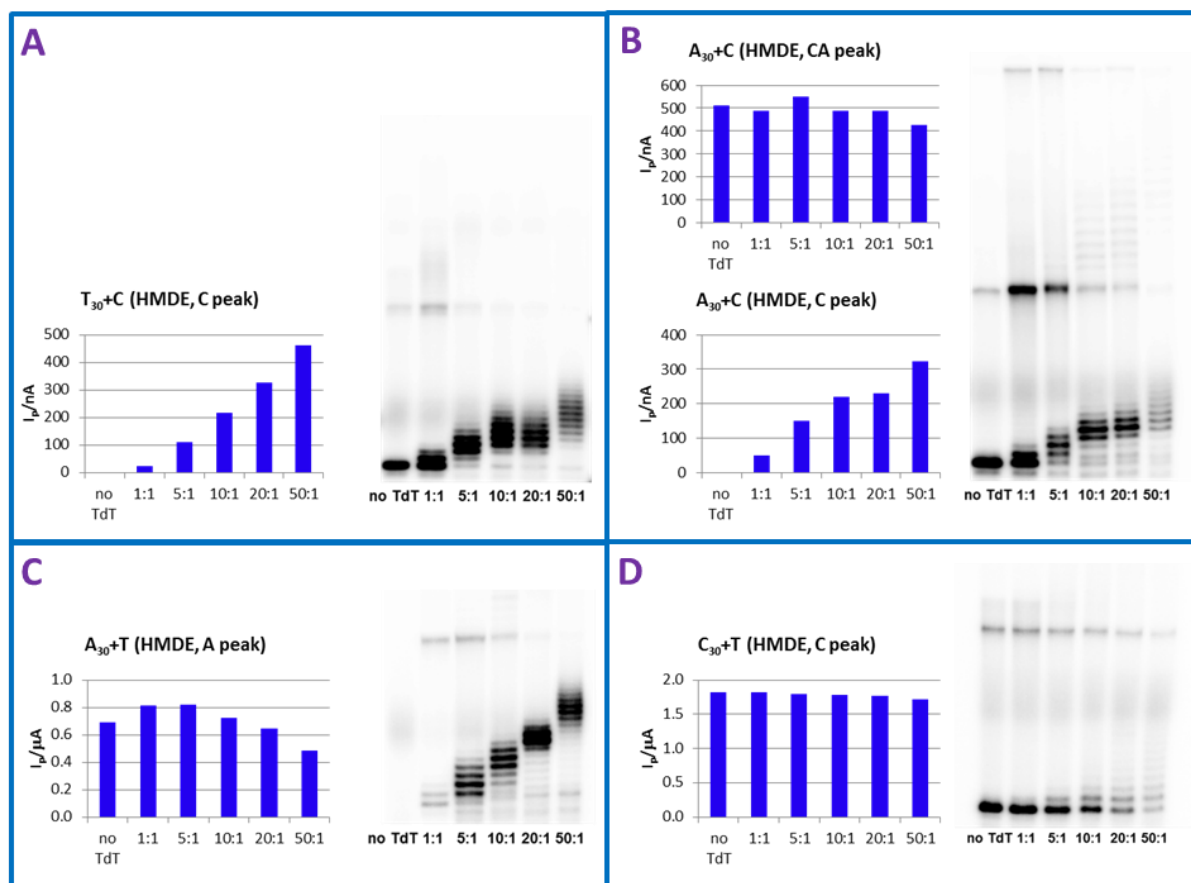
Figure 5. Heights of the respective peaks gained at HMDE and denaturing PAGE autoradiograms obtained for combinations of C and T with all three primers: (A) $T_{30}+C$; (B) $A_{30}+C$; (C) $A_{30}+T$; (D) $C_{30}+T$. Reaction conditions and significant conclusions are discussed in the text.

PAGE analysis of tailing products having tails consisting of cytosines ($T_{30}+C$ – Figure 2H and 5A and $A_{30}+C$ – Figure 2G and 5B) showed that the length of the products grows with the increasing ratio of dCTP:primer, but even at the highest ratios the products do not appear to be as long as for other bases. Since the incorporated cytosines cannot be analyzed using PGE under the used conditions, cyclic voltammetry at HMDE was used for their detection. For $T_{30}+C$, the same tensammetric peak caused by the $T_{30}$ primer ($T^{TENS}$) as in the case of $T_{30}+A$ was observed. Although $T^{TENS}$ appeared at a potential close to that of the C peak, it was possible to distinguish these two peaks as the potential at which it occurred was about 400 mV more negative than that of the C peak. The $T_{30}$ peak was clearly discernible only in the "no enzyme" control and the 1:1 ratio, with a slight hint at the 5:1 ratio; for the higher ratios the peak diminishes, indicating that with the increasing ratio of dCTP:primer, the behavior of the C-tail at the electrode surface prevails. The height of the C peak then grows gradually with the increasing ratio. In the case of $A_{30}+C$, similar situation occurred as for the $C_{30}+A$, with C and A being reduced at HMDE at close potentials. However, here it was possible to observe a separate C peak for the higher ratios of dCTP:primer. With an increasing number of cytosines forming the tail, it was observed that the C peak appeared at a less negative potential than the $A^{HMDE}$ peak. For the 50:1 ratio, the peak was already well developed. The peak heights gained

for the CA peak showed no obvious trend and remained similar for the primer and all ratios of dCTP:primer. Nevertheless, an evident tendency to be higher with the increasing ratio was seen when the C peak was analyzed separately. Moreover, this tendency matched the results gained from the PAGE analysis, with a gradual increase from the 1:1 to 10:1 ratio and further increase between 20:1 and 50:1 ratio.

Primers $A_{30}$ and $C_{30}$ were also used for tailing reaction with dTTP. The PAGE analysis of the $A_{30}$+T tailing products (Figure 5C) showed, that unlike for $T_{30}$+A, the tailing reaction was not stopped after a few added nucleotides and the tailing products gradually increased in length up to the 50:1 ratio. It remains unclear why the behavior of TdT during the $A_{30}$+T tailing reaction differs from that of the $T_{30}$+A combination. When analyzed at HMDE, the height of the A peak displayed a decreasing tendency, which reflects a decreasing amount of the $A_{30}$ parts of the tailing products that were adsorbed at the electrode surface due to a growing portion of the T-tails. The PAGE analysis of the $C_{30}$+T (Figure 5D) revealed the same problem as for the $C_{30}$+A and $C_{30}$+A* combinations – no distinct tailing products at the autoradiogram. However, the diminishing intensity of the $C_{30}$ band indicates that the tailing products were created but their length cannot be assessed. The voltammetric analysis of $C_{30}$+T at HMDE confirmed that the cytosines adsorb very strongly at the mercury surface [29], which is evident from the fact that the C peak height remains unchanged for all ratios of dTTP:primer.

Figure 6 shows the relative intensities of the peaks specific for the particular bases obtained using square wave voltammetry at PGE or cyclic voltammetry at HMDE. Values of the peak heights were normalized to the 1:1 dNTP:primer ratio, which enabled comparison of the relative signals gained for the individual combinations. The highest relative signal intensities were gained for four different combinations of primers and dNTPs – $C_{30}$+G, $C_{30}$+A, $C_{30}$+A* and $T_{30}$+C – indicating that the mutual combination of the primer and used dNTP and their ability (or ability of the tail alone) to form various structures dictate the resulting outcomes of the tailing reactions. High relative signals were also obtained for primer+dNTP combinations in which equimolar mixtures of two different dNTPs were used for the tailing reactions, suggesting that mixing two dNTPs has an impact on formation of possible DNA structures (in this case G4). Comparing the normalized $G^{HMDE}$ peak height gained for $A_{30}$+G+C and $A_{30}$+G+T, we see that unlike dCTP, adding dTTP to the reaction with dGTP did not prevent the guanines in the tail from creating the G4 structure, which is evident from the decrease of the peak height for the 50:1 ratio for the $A_{30}$+G+T products. This difference is probably caused by the ability of G and C to form duplex DNA, which reduces G stretches present in the G+C tails that would otherwise tend to form G4, and by the preference of the TdT reaction for incorporation of G in competition with T [5,6]. For more details on $A_{30}$+G+C, $A_{30}$+G+T and $A_{30}$+G*+C results, see SI.
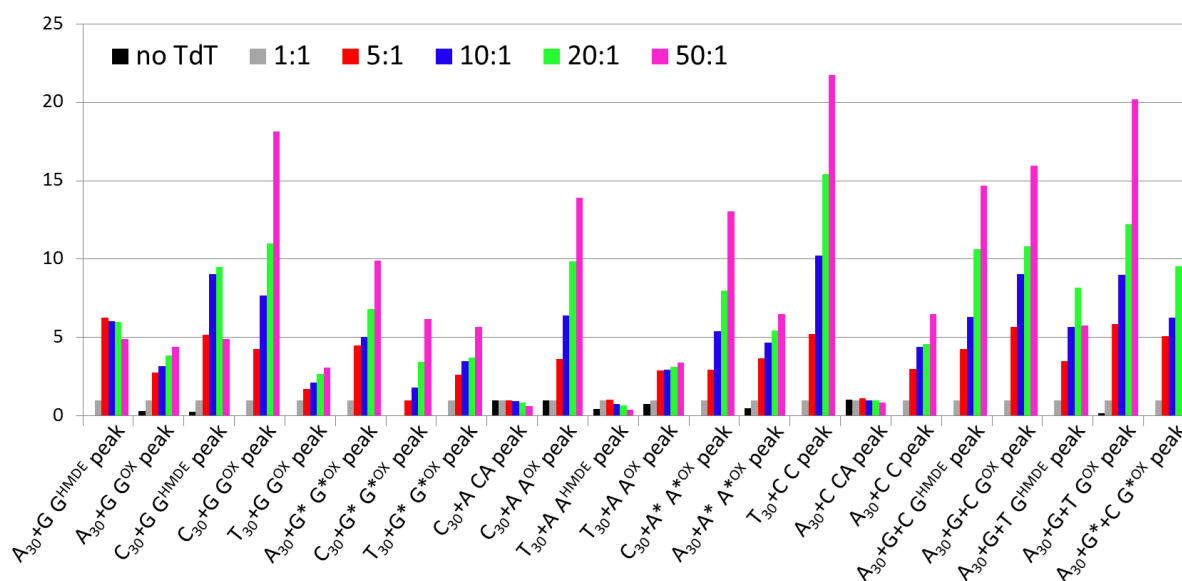
Figure 6. Normalized intensities of the respective peaks gained for all combinations of primers and dNTPs used for the TdT tailing reaction, including combinations with two mixed dNTPs ($A_{30}$+G+C, $A_{30}$+G+T and $A_{30}$+G*+C).

## 4. Conclusions

We used intrinsic electroactivity of nucleobases at HMDE and PGE to study products of the TdT tailing reactions and show that we can monitor how the tailing reaction works for various combinations of primers and dNTPs. This approach enabled study of the tailing reaction and also allowed observation of the formation of DNA structures that may affect the tailing reactions and electrochemical behavior of the respective oligonucleotides. This was particularly evident in the case of HMDE since, for all tailing products capable of forming unusual DNA structures, we observed a decrease in the corresponding signal, which reflected the structural changes and their impact on the behavior of these molecules at the negatively charged surface of HMDE. On the other hand, results obtained at PGE corresponded very precisely to those obtained using denaturing PAGE, which implies that PGE can be used for monitoring the lengths of the TdT tailing reaction products without dramatic interfering effects of secondary DNA structure. Thus, combination of measurements at both types of electrodes can provide complete (and complementary) information. In some cases, the electrochemical analysis at PGE was even more accurate than the denaturing PAGE. Thus, this approach proves to be an excellent tool for studying the TdT tailing reactions and also for exploring electrochemical behavior of the DNA oligonucleotides at electrode surfaces.

## 5. Acknowledgements

## 6. References

[1]   K.-I. Kato, J. M. Goncalves, G. E. Houts, F. J. Bollum, *J. Biol. Chem.* **1967**, *242*, 2780–2789.

[2]   E. A. Motea, A. J. Berdis, *Biochim. Biophys. Acta - Proteins Proteomics* **2010**, *1804*, 1151–1166.

[3]   D. Baltimore, *Nature* **1974**, *248*, 409–411.

[4]   F. J. Bollum, *Enzymes* **1974**, *10*, 145–171.

[5]   B. Yang, K. N. Gathy, M. S. Coleman, *J. Biol. Chem.* **1994**, *269*, 11859–11868.

[6]   M. J. Modak, *Biochemistry* **1978**, *17*, 3116–3120.

[7]   M. R. Deibel, M. S. Coleman, *J. Biol. Chem.* **1980**, *255*, 4206–12.

[8]   M. S. Chang, F. J. Bollum, *J. Biol. Chem.* **1990**, *265*, 17436–17440.

[9]   E. Paleček, *Naturwissenchaften* **1958**, *45*, 186–187.

[10]  E. Paleček, M. Bartošík, *Chem. Rev.* **2012**, *112*, 3427–3481.

[11]  M. Fojta, F. Jelen, L. Havran, E. Paleček, *Curr. Anal. Chem.* **2008**, *4*, 250–262.

[12]  J. Špaček, A. Daňhel, S. Hasoň, M. Fojta, *Electrochem. Commun.* **2017**, *82*, 34–38.

[13]  L. Trnková, M. Studničková, E. Paleček, *J. Electroanal. Chem.* **1980**, *116*, 643–658.

[14]  M. Studničková, L. Trnková, J. Zetěk, Z. Glatz, *Bioelectrochem. Bioenerg.* **1989**, *275*, 83–86.

[15]  H. Pivoňková, P. Horáková, M. Fojtová, M. Fojta, *Anal. Chem.* **2010**, *82*, 6807–6813.

[16]  M. Fojta, E. Palecek, *Anal. Chim. Acta* **1997**, *342*, 1–12.

[17]  M. Fojta, R. P. Bowater, V. Staňková, L. Havran, D. M. J. Lilley, E. Paleček, *Biochemistry* **1998**, *37*, 4853–4862.

[18]  M. Fojta, L. Havran, J. Fulnečková, T. Kubičárová, *Electroanalysis* **2000**, *12*, 926–934.

[19]  X. Cai, G. Rivas, H. Shirashi, P. Farias, J. Wang, M. Tomschik, F. Jelen, E. Paleček, *Anal. Chim. Acta* **1997**, *344*, 65–76.

[20]  A. M. Chiorcea-Paquim, A. M. Oliveira-Brett, *Electrochim. Acta* **2014**, *126*, 162–170.

[21]  P. Vidláková, H. Pivoňková, I. Kejnovská, L. Trnková, M. Vorlíčková, M. Fojta, L. Havran, *Anal. Bioanal. Chem.* **2015**, *407*, 5817–5826.

[22]  R. Roychoudhury, E. Jay, R. Wu, *Nucleic Acids Res.* **1976**, *3*, 863–77.

[23] G. Deng, R. Wu, *Nucleic Acids Res.* **1981**, *9*, 4173–4188.

[24] A. M. Michelson, S. H. Orkin, *J. Biol. Chem.* **1982**, *257*, 14773–14782.

[25] J. B. Boulé, F. Rougeon, C. Papanicolaou, *J. Biol. Chem.* **2001**, *276*, 31388–31393.

[26] J. Gouge, S. Rosario, F. Romain, P. Beguin, M. Delarue, *J. Mol. Biol.* **2013**, *425*, 4334–4352.

[27] J. Loc'h, S. Rosario, M. Delarue, *Structure* **2016**, *24*, 1452–1463.

[28] E. P. Wright, J. L. Huppert, Z. A. E. Waller, *Nucleic Acids Res.* **2017**, *45*, 2951–2959.

[29] S. Hasoň, V. Vetterl, M. Fojta, *Electrochim. Acta* **2008**, *53*, 2818–2824.

[30] Z. Dudová, J. Špaček, M. Tomaško, L. Havran, H. Pivoňková, M. Fojta, *Monatsh. Chem.* **2016**, *147*, 3–11.

[31] L. Trnková, F. Jelen, I. Postbieglová, *Electroanalysis* **2003**, *15*, 1529–1535.

[32] L. Trnková, F. Jelen, I. Postbieglová, *Electroanalysis* **2006**, *18*, 662–669.

[33] R. Mikelová, L. Trnková, F. Jelen, V. Adam, R. Kizek, *Electroanalysis* **2007**, *19*, 348–355.